Experimental and Theoretical Approach to the Understanding of $TiCl_4$ Interacting with Arenes. Isolation of a d^0-Metal–Arene Complex and Cyclotrimerization of But-2-yne Promoted by $TiCl_4$

Euro Solari,[†] Carlo Floriani,*[,†] Kurt Schenk,[‡] Angiola Chiesi-Villa,[§] Corrado Rizzoli,[§] Marzio Rosi,[∥] and Antonio Sgamellotti[∥]

Institut de Chimie Minérale et Analytique, Université de Lausanne, Place du Château 3, CH-1005 Lausanne, Switzerland, Section de Physique, Université de Lausanne, CH-1015 Lausanne, Switzerland, Istituto di Strutturistica Chimica, Centro di Studio per la Strutturistica Diffrattometrica del CNR, Università di Parma, I-43100 Parma, Italy, and Dipartimento di Chimica, Università di Perugia, I-06100 Perugia, Italy

Received June 29, 1993[⊗]

The reaction of $TiCl_4$ with C_6Me_6 in CH_2Cl_2 or 1,2-$C_6H_4Cl_2$ led to a d^0-arene complex $[(\eta^6\text{-}C_6Me_6)TiCl_3]^+[Ti_2Cl_9]^-$ (**2**), which was structurally characterized by an X-ray analysis. The structure consists of a three-leg piano-stool metallic fragment $(TiCl_3)^+$ η^6 binding the arene moiety. The ^1H NMR spectrum of the reaction solution indicated the presence of a charge transfer intermediate. The high stability of **2** is evidenced by the $TiCl_4$-promoted stoichiometric cyclotrimerization of but-2-yne. The theoretical calculations on the model compounds $[(\eta^6\text{-}C_6H_6)TiX_3]^+$ (X = H, F, Cl) and $[(\eta^6\text{-}C_6H_6)TiX_3]$ (X = F, Cl) explain the high stability of the titanium(IV) derivatives, as well as the weaker arene–metal interaction in the titanium(III) derivatives. Also, a strong positive charge was found on the benzene hydrogens, consistent with an electrophilic activation of the benzene ring. Theoretical calculations have been carried out on some possible precursors to **2**, like $[(\eta^6\text{-}C_6H_6)TiCl_4]$, $[(\eta^2\text{-}C_6H_6)TiCl_4]$, and $[Cl_3Ti\text{–}Cl\cdots\eta^6\text{-}C_6H_6]$. Crystallographic details: **2** is orthorhombic, space group $Pca2_1$, with a = 17.263(2) Å, b = 8.712(1) Å, c = 17.256(2) Å, $\alpha = \beta = \gamma = 90°$, Z = 4, and R = 0.059.

Introduction

Titanium tetrachloride is a widely used Lewis acid for a variety of metal-assisted organic reactions.[1] Studies on the interaction between $TiCl_4$ and organic substrates containing basic sites date back a long time.[2] The evidence for the interaction of $TiCl_4$ with hydrocarbons and particularly aromatic hydrocarbons[3] is mainly spectroscopic,[4] without the isolation and characterization of any compound. A yellow solid was reported to form from a CCl_4 solution of C_6Me_6 with an excess of $TiCl_4$.[5] The solid had a $C_6Me_6{\cdot}2TiCl_4$ stoichiometry, which does not correspond to what we have isolated and structurally characterized.[5] The recent isolation of η^6-arene compounds of the f-block[6] elements and tin(II)[7] encouraged us in the search for M(IV)-d^0 (M = Ti, Zr, Hf) arene complexes. From these compounds we would expect the following: (i) information on the nature of the charge transfer complexes formed from high-valent metal halides and aromatic hydrocarbons; (ii) the redox properties, which, in case of $TiCl_4$–aromatic hydrocarbons, were recently studied by Kochi and coworkers;[4] (iii) the electrophilic activation of an arene; (iv) the generation of highly acidic metals in noncoordinating solvents.

We report the reaction between $TiCl_4$ with hexamethylbenzene in chlorinated solvents giving $[(\eta^6\text{-}C_6Me_6)TiCl_3]^+[Ti_2Cl_9]^-$, which contains the strongly acidic $[TiCl_3]^+$ fragment.[8] This reaction was monitored *via* ^1H NMR spectroscopy. The high stability of $[(\eta^6\text{-}C_6Me_6)TiCl_3]^+$ is a likely driving force of the cyclotrimerization of but-2-yne in the presence of an unusual promoter like $TiCl_4$. Examples of d^0-metal–arene complexes in the literature are rare[8,9] and include the zwitterionic compound $[(\eta^6\text{-}C_6H_5PBh_3)Zr(CH_2Ph)_3]$[10] and $[cp^*MMe_2(\eta^6\text{-arene})][BMe(C_6F_5)_3]$[11] [M = Ti, Zr, Hf; $cp^* = \eta^5\text{-}C_5Me_5$].

* To whom correspondence and reprint requests should be addressed.
† Institut de Chiie Minérale et Analytique, Université de Lausanne.
‡ Section de Physique, Université de Lausanne.
§ Università di Parma.
∥ Università di Perugia.
⊗ Abstract published in *Advance ACS Abstracts,* April 1, 1994.

(1) (a) Shambayati, S.; Schreiber, S. In *Comprehensive Organic Synthesis*; Trost, B. M., Fleming, I., Eds.; Pergamon: Oxford, U.K.; Vol. 1; p 283. (b) Baaz, M.; Gutmann, V. In *Friedel-Crafts and Related Reactions*; Olah, G. A., Ed.; Wiley: New York, 1963; Vol. 1. (c) DeHaan, F. P.; Chan, W. H.; Chang, J.; Cheng, T. B.; Chiriboga, D. A.; Irving, M. M.; Kaufman, C. R.; Kim, G. Y.; Kumar, A.; Na, J.; Nguyen, T. T.; Nguyen, D. T.; Patel, B. R.; Sarin, N. P.; Tidwell, J. H. *J. Am. Chem. Soc.* **1990**, *112*, 356. (d) Corcoran, R. C.; Ma, J. *J. Am. Chem. Soc.* **1991**, *113*, 3973. (e) Oppolzer, W.; Rodriguez, I.; Blagg, J.; Bernardinelli, G. *Helv. Chim. Acta* **1989**, *72*, 123. Roll, T.; Metter, J. O.; Helmchen, G. *Angew. Chem., Int. Ed. Engl.* **1985**, *24*, 112. Kunz, H.; Muleer, B.; Schanzenbach, D. *Angew. Chem., Int. Ed. Engl.* **1987**, *86*, 867. (f) Benner, J. P.; Gill, G. B.; Parrot, S. J.; Wallace, B. *J. Chem. Soc., Perkin Trans.* **1984**, *1*, 291. Whitesell, J. K.; Madley, S. W.; Kelly, J. D.; Bacon, E. R.; *J. Org. Chem.* **1985**, *50*, 4144. (g) Hosomi, A.; Imai, T.; Endo, M.; Sakurai, H. *J. Organomet. Chem.* **1985**, *285*, 95. Bartlett, P. A.; Johnson, W. S.; Elliott, D. J. *J. Am. Chem. Soc.* **1983**, *105*, 2088. Heathcock, C. H.; Kydoka, S.; Blumenkoff, D. A. *J. Org. Chem.* **1984**, *49*, 4214. (h) Danishefsky, S. J.; Pearson, W. H.; Harvey, D. F. *J. Am. Chem. Soc.* **1984**, *106*, 2455. Danishefsky, S. J.; Pearson, W. H.; Miles, D. C. *J. Am. Chem. Soc.* **1987**, *109*, 862. (i) Mukaiyama, T.; Narasaka, K.; Banno, K. *J. Am. Chem. Soc.* **1974**, *96*, 7503. Gennari, C.; Bernardi, A.; Colombo, L.; Scolastico, C. *J. Am. Chem. Soc.* **1985**, *107*, 5812. Reetz, M. T. *Angew. Chem., Int. Ed. Engl.* **1984**, *23*, 556. Heathcock, C. H.; Davidsen, S. K.; Hug, K. T.; Flippin, L. A. *J. Org. Chem.* **1986**, *51*, 3027.

(2) McAuliffe, C. A. In *Comprehensive Coordination Chemistry*, Wilkinson, G., Gillard, R. D., McCleverty, J. A., Eds.; Pergamon: Oxford, U.K., 1987; Vol. 3; Chapter 31. Fay, R. C. *Coord. Chem. Rev.* **1981**, *27*, 9.

(3) (a) For a summary, see: Perkampus, H. H. *Wechselwirkung von π-Elektronensystemen mit Metallhalogeniden*; Springer: New York, 1973; p 86 ff. (b) Elliott, B.; Evans, A. G.; Owen, E. D. *J. Chem. Soc.* **1962**, 689. (c) Brackman, D. S.; Plesh, P. H. *J. Chem. Soc.* **1953**, 1289. (d) Dijkgraaf, J. C. *Spectrochim. Acta* **1965**, *21*, 769. (e) Dijkgraaf, J. C. *J. Phys. Chem.* **1965**, *69*, 660. (f) Hammond, P. R. *J. Chem. Soc. A* **1971**, 3826 and references in preceeding papers of the series.

(4) Brügermann, K.; Czernuszewicz, R. S.; Kochi, J. K. *J. Phys. Chem.* **1992**, *96*, 4405.

(5) Krauss, H. L.; Hüttman, H. *Z. Naturforsch.* **1963**, *18b*, 976.

(6) Cesari, M.; Pedretti, U.; Zazzetta, A.; Lugli, G.; Marconi, N. *Inorg. Chim. Acta* **1971**, *5*, 439. Cotton, F. A.; Schwotzer, W. *Organometallics* **1985**, *4*, 942. Campbell, G. C.; Cotton, F. A.; Haw, J. F.; Schwotzer, W. *Organometallics* **1986**, *5*, 274. Cotton, F. A.; Schwotzer, W.; Simpson, C. Q. *Angew. Chem., Int. Ed. Engl.* **1986**, *25*, 637. Cotton, F. A.; Schwotzer, W. *J. Am. Chem. Soc.* **1986**, *108*, 4657. Baudry, D.; Bulot, E.; Charpin, P.; Ephritikhine, M.; Lance, M.; Nierlich, M.; Vigner, J. *J. Organomet. Chem.* **1989**, *371*, 155.

(7) Schmidbaur, H.; Probst, T.; Huber, B.; Steingelmann, O.; Müller, G. *Organometallics* **1989**, *8*, 1567 and references therein.

(8) Some of these results have been briefly communicated: Solari, E.; Floriani, C.; Chiesi-Villa, A.; Guastini, C. *J. Chem. Soc., Chem. Commun.* **1989**, 1747.

(9) Floriani, C.; Berno, P.; Solari, E. *Chem. Scr.* **1989**, *29*, 423.

0020-1669/94/1333-2018$04.50/0

We completed our investigation by a theoretical study of the η^6 interaction mode of C_6H_6 with a series of $[TiX_3]^+$ cations (X = H, F, Cl) and the corresponding titanium(III) fragments in the hypothetical compounds $[(\eta^6\text{-}C_6H_6)TiX_3]$ (X = F, Cl). The latter forms may be related to redox species involved in MCl_4–arene charge-transfer complexes.[4] The study includes calculations on some plausible precursors to the isolated (η^6-arene)titanium compound.

Experimental Section

All the reactions were carried out under an atmosphere of purified nitrogen. Solvents were dried and distilled by standard methods before use. Infrared spectra were recorded on a Perkin-Elmer 883 spectrophotometer and ^1H NMR spectra on a 200-AC Bruker instrument.

Reaction between $TiCl_4$ and C_6Me_6. Synthesis of 2. $TiCl_4$ (20 mL, 182.4 mmol) was added to a CH_2Cl_2 (100 mL) solution of C_6Me_6 (5.00 g, 30.81 mmol). The colorless solution turned deep red-violet and within a few minutes a yellow crystalline solid formed. The solid was washed with CH_2Cl_2 and dried in vacuo (70.2%) Anal. Calcd for $[(\eta^6\text{-}C_6Me_6)TiCl_3][Ti_2Cl_9]$, $C_{12}H_{18}Cl_{12}Ti_3$: C, 19.71; H, 2.48; Cl, 58.17; Ti, 19.64. Found: C, 19.15; H, 2.48; Cl, 57.71; Ti, 19.65. The same reaction was carried out in both *n*-hexane and 1,2-dichlorobenzene following the same procedure. A very crucial factor is the $TiCl_4/C_6Me_6$ ratio, which should be higher than 3. Crystals suitable for X-ray analysis were prepared in the drybox using the following procedure: $TiCl_4$ (5.0 mL, 45.60 mmol) was added to a solution in 1,2-dichlorobenzene (20 mL) of C_6Me_6 (2.0 g, 12.32 mmol). The resulting suspension was heated up to form a deep-brown solution, which was left to cool to room temperature over a period of 3 days. Yellow crystals formed, but were unsuitable for an X-ray analysis. The solution was transferred to an empty flask and upon standing for 1 week gave crystals suitable for the X-ray analysis.

A quantitative decomposition of **2** with dry THF in *n*-hexane was carried out. A suspension of **2** (2.89 g, 3.96 mmol) in *n*-hexane (30 mL) was treated with THF (10.0 mL) and then stirred for 12 h. The solid formed $TiCl_4{\cdot}THF_2$ (3.85 g, 11.53 mmol) was filtered out and washed with *n*-hexane; the *n*-hexane solution was found (by GC) to contain only C_6Me_6 (0.625 g, 3.86 mmol). Analogous quantitative decomposition of the suspension derived from the reaction of $TiCl_4$ with C_6Me_6 in CH_2Cl_2 gave quantitatively and exclusively $TiCl_4{\cdot}THF_2$ and C_6Me_6, when treated with THF.

^1H NMR Inspection on the Reaction between $TiCl_4$ and C_6Me_6.

(1) The ^1H NMR spectra were recorded for different $TiCl_4/C_6Me_6$ molar ratios in CD_2Cl_2, and at different temperatures. The results are listed as follows.

(i) C_6Me_6 (0.030 g, 0.185 mmol) dissolved in CD_2Cl_2 (0.60 mL) has a singlet at 293 K at δ 2.21 ppm.

(ii) $TiCl_4$ (0.035 g, 0.185 mmol) was added to a solution of C_6Me_6 (0.030 g, 0.185 mmol) in CD_2Cl_2 (0.60 mL). The molar ratio is 1:1, and we did not observe and solid forming. The spectrum at 283 K shows sharp singlets at 2.83 and 2.22 ppm. The intensity of the signal at 2.83 ppm decreases considerably at 303 K and disappears at 323 K.

(iii) $TiCl_4$ (0.105 g, 0.56 mmol) was added to a solution of C_6Me_6 (0.030 g, 0.185 mmol) in CD_2Cl_2 (0.60 mL). This is a solution at 283 K and at higher temperatures. The molar ratio is 3:1. The spectrum at 283 K shows singlets at 2.83 (strong), 2.75 (very weak), and 2.22 ppm. The intensity of the singlets at 2.83 and 2.75 ppm decreases with increasing temperature, until disappearing at 323 K, while an increase is observed for the free C_6Me_6 at 2.22 ppm.

(iv) $TiCl_4$ (0.21 g, 1.11 mmol) was added to a solution of C_6Me_6 (0.030 g, 0.185 mmol) in CD_2Cl_2 (0.60 mL). In this case (6:1 molar ratio) the yellow solid **2** forms at room temperature, but it does not interfere with a correct NMR analysis since it floats on the dense solution. The spectrum at 283 K shows singlets at 2.83, 2.75 (very weak), and 2.22 ppm; at 303 K the intensity of the singlet at 2.83 ppm increases considerably and then decreases almost to the point of disappearance at 323 K (complete dissolution of the solid). At 303 K the increase in the temperature has more influence on increasing the solubility of **2** than to regress the equilibrium shown in eq 4.

(v) $TiCl_4$ (0.385 g, 2.04 mmol) was added to a solution of C_6Me_6 (0.030 g, 0.185 mmol) in CD_2Cl_2 (0.60 mL). In this case (11:1 molar ratio) we have a large amount of solid **2**. The spectrum at 293 K, with the solid floating on the solution, shows two intense singlets at 2.83 and 2.22 ppm and a weak singlet at 2.75 ppm. At temperatures from 323 to 343 K, we observed a significant decrease of the singlet at 2.83 ppm and disappearance of the peak at 2.75 ppm, while the peak C_6Me_6 at 2.22 ppm increases significantly.

(2) The following ^1H NMR spectra have been recorded by adding increasing amounts of C_6Me_6 to a CD_2Cl_2 solution of **2**. Complex **2** (0.058 g, 0.079 mmol) dissolved completely in CD_2Cl_2 (0.60 mL) at 278 K. At lower temperatures **2** is not completely soluble. The spectrum at 278 K shows singlets at 2.82, 2.75 (weak), and 2.20 ppm; at 303 K the intensity of the singlet at 2.83 ppm decreases considerably and that at 2.75 disappears, while a significant increase is observed the free C_6Me_6 at 2.22 ppm. At 323 K a single strong singlet is present at 2.22 ppm.

The addition of increasing amounts of free C_6Me_6 (0.06, 0.24, and 0.43 mmol) to the solution of **2** above 283 K resulted, as a major feature, in a significant decrease of intensity of the singlets at 2.83 and 2.75 ppm.

(3) We should add a few remarks concerning the NMR investigation above.

(i) At very low concentration of **2** at 283 K (i.e. 0.010 g, 0.014 mmol in 0.60 mL of CD_2Cl_2), we did not detect the peaks at 2.83 and 2.75 ppm.

(ii) Owing to the very high difference in the intensity between the various singlets, a quantitative ratio might not be assessed.

(iii) Some significant shifts depending on the concentration have been observed for the singlets at 2.83, 2.75, and 2.22 ppm, though we considered average values.

All the above experiments have been performed using benzene instead of C_6Me_6. In these cases, no solid forms, and no change in the ^1H NMR is detectable.

Reaction between $TiCl_4$ and MeC≡CMe. $TiCl_4$ (30 mL, 273.60 mmol) was added to a CH_2Cl_2 (100 mL) solution of Me_2C_2 (3.0 mL, 38.26 mmol). The solution turned yellow, and the color gradually became deeper in intensity. A yellow crystalline solid started crystallizing after 24 h (61.3%). The ^1H NMR spectrum in CD_2Cl_2 revealed the presence of C_6Me_6 (δ, 2.22 ppm). The reaction can be carried out in an NMR tube in CD_2Cl_2 with variable $TiCl_4$/but-2-yne molar ratios. The peaks at δ 2.22 (C_6Me_6) and 2.83 ppm (complex **2**) appear after 2 days standing. Hydrolysis gave C_6Me_6 (GC). In 1 week, crystals formed, which were found to be the same as complex **2** by X-ray diffraction. The reaction between $TiCl_4$ and Me_2C_2 has also been carried out in 1,2-dichlorobenzene with the same results (yield 60%). The conversion of but-2-yne has never been catalytic under the conditions we used or in any other attempt we made.

Computational Details

Basis Sets. The s, p basis for titanium is taken from the (12s6p4d) set of ref 12 with the addition of two basis functions to describe the 4p orbital,[13] while the outermost diffuse s function is deleted. The Ti d basis is the reoptimized (5d) set of ref 14, contracted 4/1. This leads to an (11s8p5d) primitive basis for titanium, contracted to [8s6p2d]. A (9s5p)/[3s2p] contraction is used for carbon and fluorine,[15] while a (11s7p)/[6s4p] basis is used for chlorine.[15] The (4s)/[2s] basis of Dunning and Hay[15] is used for hydrogen, with a scale factor of 1.2. This basis set will be called hereafter basis **I**.

A second basis set is derived from basis **I** with the addition of a diffuse p function, provided in ref 15 for the description of negative ions, to augment the basis of fluorine and chlorine. This basis will be called hereafter basis **II**.

A third basis set is derived considering the (14s11p5d)/[10s8p2d] set of ref 14 for titanium, the (10s6p)/[5s3p] set of ref 16 for fluorine, and the (12s9p)/[6s5p] of ref 17 for chlorine. This basis set is augmented for all the atoms with the polarization d function recommended by Ahlrichs and Taylor.[18] This basis set will be called hereafter basis **III**.

In the last basis set (hereafter called basis **IV**), for titanium we use the [8s4p3d] contraction of the (14s9p5d) primitive Gaussian basis set of Wachters[19] supplemented with two diffuse p functions and a diffuse

(10) Bochmann, M.; Karger, G.; Jaggar, A. J. *J. Chem. Soc., Chem. Commun.* **1990**, 1038.
(11) Gillis, D. J.; Tudoret, M. J.; Baird, M. C. *J. Am. Chem. Soc.* **1993**, *115*, 2543.
(12) Roos, R.; Veillard, A.; Vinot, G. *Theor. Chim. Acta* **1971**, *20*, 1.
(13) Hood, D. M.; Pitzer, R. M.; Schaefer, H. F., III. *J. Chem. Phys.* **1979**, *71*, 705.
(14) Rappe, A. K.; Smedley, T. A.; Goddard, W. A., III. *J. Phys. Chem.* **1981**, *85*, 2607.
(15) Dunning, T. H., Jr.; Hay, P. J. In *Modern Theoretical Chemistry*, Schaefer, H. F., III, Ed.; Plenum: New York, 1977; Vol 3; p 1.
(16) Dunning Jr., T. H. *J. Chem. Phys.* **1971**, *55*, 716.
(17) McLean, A. D.; Chandler, G. S. *J. Chem. Phys.* **1980**, *72*, 5639.
(18) Ahlrichs, R.; Taylor, P. R. *J. Chim. Phys.* **1981**, *78*, 315.

d function.[20] This is further augmented by a single contracted set of f polarization functions, which is based on a three-term fit[21] to a Slater-type orbital, with exponent of 2.0. This is a 3d correlating function rather than a true polarization function. The final Ti basis is of the form (14s11p6d3f)/[8s6p4d1f]. The F and Cl basis sets are the same used in basis III. In the calculations performed with basis IV, only the pure spherical harmonic components of the basis functions are used.

The structures of TiF_3^+ and $TiCl_3^+$ have been investigated using all the above-described basis sets, as explained in the text, while the calculations in the other systems have been performed using basis I.

Methods. All calculations use the size-consistent modified coupled pair (MCPF) functional method,[22] which uses an SCF zeroth-order wave function. In all the analyzed systems, the SCF occupation is a good zeroth-order representation; thus, the use of the MCPF approach is valid. All the valence electrons (55 for the largest system) are correlated. When so many electrons are correlated, a size-consistent method becomes essential and this supports our choice of the MCPF approach. In the MCPF calculations for the open-shell systems we impose the first-order interacting space restriction[23] to reduce the CI expansion length. This is not expected to affect the accuracy of the computer binding energy values. All calculations were performed on the CRAY Y-MP 8/464 computer of the CINECA computing center using the MOLECULE-SWEDEN[24] and GAMESS-UK[25] program systems.

Geometries and Geometry Optimization. Full geometry optimizations are performed through gradient SCF calculations for $TiX_3^{0,+}$ (X = F, Cl) and C_6H_6, with only the following restriction of the symmetry: C_{3v} or D_{3h} and D_{6h}, respectively. For $TiX_3^{0,+}$ the optimization is performed for both the planar and nonplanar geometries. For $TiX_3C_6H_6^{0,+}$, we optimize the three geometrical parameters r(Ti–X), $\angle$(XTiX), and r(Ti–C^n), where C^n refers to the centroid of C_6H_6, using gradient SCF calculations. The r(C–C) bond distance is taken from the X-ray structure of $[(\eta^6\text{-}C_6Me_6)TiCl_3]^+[Ti_2Cl_9]^-$,[8] while the r(C–H) bond length is taken from the experimental geometry of benzene.[26] This choice is checked by performing a full geometry optimization on $TiCl_3C_6H_6^+$. The geometry of $TiCl_4C_6H_6$ is optimized assuming both a trigonal bipyramid and a square base pyramid with the benzene ring occupying the apex site. A structure of $TiCl_4C_6H_6$ with a chlorine atom pointing toward the center of the benzene ring has been as well studied. In the investigation of the inversion barriers for TiF_3^+ and $TiCl_3^+$ and in the trimerization reaction of the acetylene, transition state locations are performed through the synchronous transit method.[27] In order to get zero point energies for TiF_3^+, force constants, together with the associated vibrational frequencies, are calculated by taking finite differences of gradients, at the SCF level. Some geometrical parameters are reoptimized at a higher level of theory and the minimum is obtained by fitting the computed energy points to be a polinomial.

X-ray Crystallography.[28] Intensity data were collected at room temperature on a single-crystal four-circle diffractometer. Crystal data and details of the parameters associated with data collection and structure refinement are given in Tables 1 and S2. The reduced cell quoted was obtained with use of TRACER.[29] For intensities and background, individual reflection profiles were analyzed.[30] The structure amplitudes were obtained after the usual Lorentz and polarization corrections. No corrections for absorption was applied. The function minimized during the full-matrix least-squares refinement was $\sum w|\Delta F|^2$. Unit weights were applied: Anomalous scattering corrections were included in all structure factor calculations.[31b] Scattering factors for neutral atoms were taken from ref 31a for non hydrogen atoms and from ref 32 for H. Among the low-angle reflections, no correction for secondary extinction was deemed necessary.

Table 1. Crystallographic Data for Complex **2**

chem formula: $C_{12}H_{18}Cl_3Ti{\cdot}Cl_9Ti_2$	space group: $Pca2_1$
a = 17.263(2) Å	T = 22 °C
b = 8.712(1) Å	λ = 0.710 69 Å
c = 17.256(2) Å	ρ_{calc} = 1.872 g cm^{-3}
V = 2595.2(5)°	μ = 21.44 cm^{-1}
Z = 4	transm coeff = 0.785–1.000
fw = 731.4	R^a = 0.059

^{a} $R = \sum|\Delta F|/\sum|F_o|$.

Table 2. Fractional Atomic Coordinates (×10^4) for Complex **2**

atom	x/a	y/b	z/c
Ti1	3057(1)	3598(3)	8185(–)
Ti2	839(1)	7920(3)	6060(2)
Ti3	–259(1)	10503(3)	5080(2)
Cl1	1158(2)	9922(4)	5112(3)
Cl2	–240(2)	7633(4)	5128(3)
Cl3	–21(2)	10004(4)	6493(2)
Cl4	283(2)	6291(5)	6878(3)
Cl5	1750(2)	8753(4)	6864(3)
Cl6	1544(3)	6228(5)	5431(3)
Cl7	–261(3)	10503(5)	3813(3)
Cl8	–1520(2)	10520(5)	5298(3)
Cl9	–25(2)	12956(4)	5292(3)
Cl10	4149(2)	4568(5)	8593(3)
Cl11	3410(3)	1529(5)	7584(3)
Cl12	2553(3)	2698(6)	9254(3)
C1	2538(7)	6299(14)	8081(7)
C2	1903(7)	5335(13)	8221(7)
C3	1734(8)	4129(13)	7726(8)
C4	2193(7)	3884(15)	7029(7)
C5	2827(7)	4813(15)	6897(7)
C6	3012(7)	6053(14)	7434(7)
C7	2692(11)	7643(17)	8608(10)
C8	1366(10)	5612(20)	8909(10)
C9	1024(10)	3063(19)	7892(11)
C10	1952(11)	2718(17)	6450(9)
C11	3310(10)	4639(22)	6171(9)
C12	3698(10)	7073(17)	7273(10)

The number of molecules per unit cell (Z = 4) required the molecules to possess an imposed crystallographic symmetry ($C2$ or m) in the centrosymmetric space groups *Pbma* or to be in general positions in the noncentrosymmetric space group $Pca2_1$. With this in mind we tried to solve the structure in the centrosymmetric space group either with direct methods or with the heavy atom method, but we did not succeed. The structure was then solved in the noncentrosymmetric space group by the heavy atom method from the vector distributions of the Patterson map. The successful solution of the structure confirmed the noncentrosymmetric space group since the local symmetry shown by anions and cations is not amenable to the crystallographic symmetry required by the centrosymmetric space group, i.e. the coordinates cannot be transformed to *Pbma*. Refinement was first done isotropically, then anisotropically for all the non-H atoms. All the hydrogen atoms were put in geometrically calculated positions and introduced in the refinement as fixed contributors (U_{iso} = 0.05 Å^2). The final difference map showed no unusual feature, with no significant peak above the general background. Final atomic coordinates, thermal parameters, bond distances, and bond angles are given in Tables 2, S3, S4, and S5.

Results

Though it has long been accepted that the solutions resulting from $TiCl_4$/aromatic hydrocarbon mixtures owe their colors to charge transfer complexes, there is little direct evidence for these

(19) Wachters, A. J. H. *J. Chem. Phys.* **1970**, *52*, 1033.
(20) Hay, P. J. *J. Chem. Phys.* **1977**, *6*, 4377.
(21) Stewart, R. F. *J. Chem. Phys.* **1970**, *52*, 431.
(22) Chong, D. P.; Langhoff, R. S. *J. Chem. Phys.* **1986**, *84*, 5606. See also: Ahlrichs, R.; Scharf, P.; Ehrhardt, C. *J. Chem. Phys.* **1985**, *82*, 890.
(23) Bunge, A. *J. Chem. Phys.* **1953**, *70*, 20. Bender, C. F.; Schaefer, H. F. III. *J. Chem. Phys.* **1971**, *55*, 7498. McLean, A. D.; Liu, B. *J. Chem. Phys.* **1973**, *58*, 1066.
(24) Almlöf, J.; Bauschlicher, C. W.; Blomberg, M. R. A.; Chong, D. P.; Heiberg, A.; Langhoff, S. R.; Malmqvist, P.-A.; Rendell, A. P.; Ross, B. O.; Siegbahn, P. E. M.; Taylor, P. R. MOLECULE-SWEDEN, an electronic structure program system.
(25) Guest, M. F.; Sherwood, P. *GAMESS-UK, User's Guide and Reference Manual*; SERC Daresbury Laboratory: Daresbury, U.K., 1992.
(26) Herzberg, G. *Molecular Spectra and Molecular Structure*; Van Nostrand Reinhold Co.: New York, 1966; Vol 3.
(27) Bell, S.; Crighton, J. S. *J. Chem. Phys.* **1984**, *80*, 2464.
(28) Data reduction, structure solution, and refinement were carried out on a GOULD 32/77 computer using: Scheldrick, G. *SHELX-76: System of Crystallographic Computer Programs*; University of Cambridge: Cambridge, England, 1976.
(29) Lawton, S. L.; Jacobson, R. A. *TRACER, a cell reduction program*; Ames Laboratory. Iowa State University of Science and Technology: Ames, IA, 1965.
(30) Lehmann, M. S.; Larsen, F. K. *Acta Crystallogr., Sect. A: Cryst. Phys. Diffr., Theor. Gen. Crystallogr.* **1974**, *A30*, 580–584.
(31) *International Tables for X-ray Crystallography*; Kynoch Press: Birmingham, England, 1974; Vol IV: (a) p 99; (b) p 149.
(32) Stewart, R. F.; Davidson, E. R.; Simpson, W. T. *J. Chem. Phys.* **1965**, *42*, 3175.

complexes.[3-7] We attempted to isolate and raise spectroscopic evidence for some intermediate species.

From a variety of possibilities, we first choose to inspect the reaction of C_6Me_6 with $TiCl_4$ in chlorinated solvents, such as CH_2Cl_2 and 1,2-$C_6H_4Cl_2$. This reaction was briefly investigated several years ago using CCl_4 as solvent, and a $TiCl_4/C_6Me_6$ 2:1 adduct was isolated.[5] The stoichiometry of the adduct is different from the adduct we have isolated in other solvents.

The reaction between $TiCl_4$ and C_6Me_6 carried out in either CD_2Cl_2 or 1,2-$C_6H_4Cl_2$ in the conditions specified in the Experimental Section, led to the isolation of **2** as a yellow crystalline solid.

$$C_6Me_6 + TiCl_4 \rightleftharpoons [C_6Me_6 \cdot TiCl_4] \xrightleftharpoons{TiCl_4} \underset{\mathbf{2}}{[(\eta\text{-}C_6Me_6)TiCl_3]^+}\,Ti_2Cl_9^- \qquad (1)$$

$$\underset{\mathbf{1}}{[C_6Me_6 \cdot TiCl_4]}$$

Complex **2** has been fully characterized including the X-ray analysis. In order to exclude the presence in the solid formed in reaction 1 of compounds other than **2**, we carried out its decomposition with THF in *n*-hexane. We obtained quantitatively $TiCl_4 \cdot THF_2$ and C_6Me_6. The ^1H NMR spectrum of **2** dissolved in CD_2Cl_2 at 278 K shows three singlets at 2.83 (strong), 2.75 (weak), and 2.22 (strong) ppm. In order to understand the feature of such a spectrum the reaction of $TiCl_4$ with C_6Me_6 in CD_2Cl_2 was followed at room temperature *via* ^1H NMR spectroscopy, as a function of the $TiCl_4/C_6Me_6$ ratio and at variable temperature. These measurements have been detailed in the experimental section. They have been carried out essentially following two procedures: (1) adding increasing amounts of $TiCl_4$ to a CD_2Cl_2 solution of C_6Me_6; (2) adding increasing amounts of C_6Me_6 to a solution of complex **2** in CD_2Cl_2. The conclusions which can be drawn from these data can be summarized as follows.

(i) Under the most general conditions three singlets in the ^1H NMR spectrum are simultaneously observed, at 2.83, 2.75, and 2.22 ppm. The first one (2.83 ppm) belongs to complex **2** and the last one (2.22 ppm) to the free C_6Me_6, and they are by far the most significant ones. The other one at 2.75 ppm constantly present, even though rather weak, can be detected only under carefully controlled solution concentrations. The relative intensity of the three singlets depends on the reagents ratio and on the temperature.

(ii) Some of the measurements have been carried out in the presence of solid **2**, but this did not interfere, since the solid floats on the solution.

(iii) The effect on all solutions of increasing the temperature is to shift the system toward the free C_6Me_6, with the singlets at 2.83 and 2.75 ppm decreasing and the other at 2.22 ppm increasing in intensity.

The results reported in eq 1 have been obtained only with C_6Me_6. With benzene, we observed neither the same spectroscopic results nor the separation of a solid under the same conditions. This does not exclude the formation of titanium–benzene complexes, which we were not able to detect.

The structure of the cation and the anion in complex **2** are shown in Figures 1 and 2, while a selection of structural parameters is reported in Table 3. The overall structure of the cation can be described as a three-legged piano stool, with the Cl–Ti–Cl angles being essentially equal and averaging 102.8(3)°. The Ti–C^n (centroid of C_6Me_6) [2.085(12) Å in complex **2**] is long compared to η^6-arene complexes of titanium in lower oxidation states: $[Ti(\eta^6\text{-}C_6Me_6)_2]$ (1.736 Å),[33] $[Ti(\eta^6\text{-}PhC_6H_5)_2]^-$ (1.78-

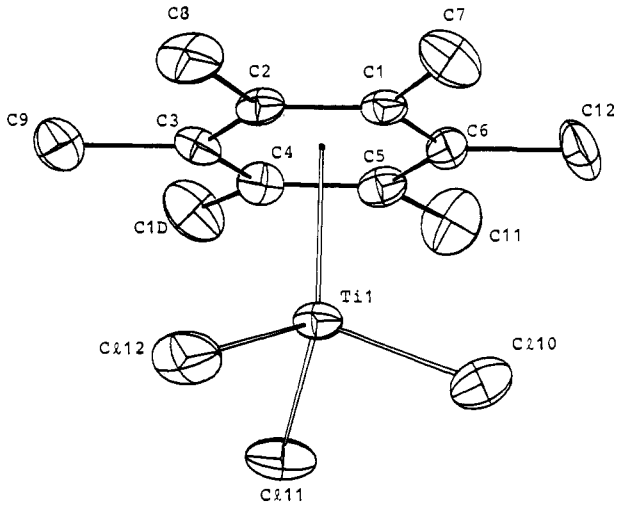

Figure 1. ORTEP drawing of the $[(\eta\text{-}C_6H_6)TiCl_3]^+$ cation (35% probability ellipsoids).

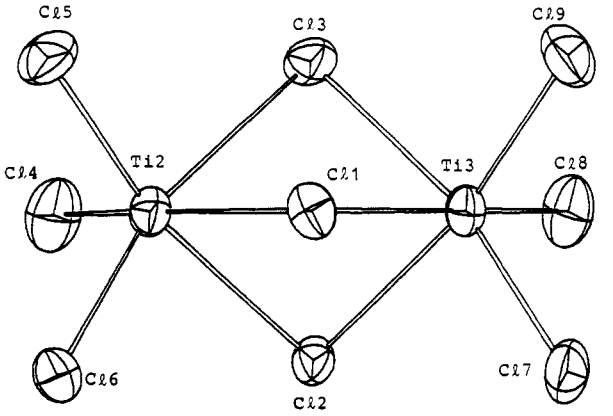

Figure 2. ORTEP drawing of the $[Ti_2Cl_9]^-$ anion (35% probability ellipsoids).

Table 3. Selected Bond Distances (Å) and Angles (deg) for Complex **2**[a]

Ti1–Cl10	2.182(4)	Ti2–Cl3	2.461(4)
Ti1–Cl11	2.168(4)	Ti2–Cl4	2.220(5)
Ti1–Cl12	2.186(5)	Ti2–Cl5	2.220(5)
Ti1–C1	2.524(12)	Ti2–Cl6	2.198(5)
Ti1–C2	2.501(12)	Ti3–Cl1	2.497(3)
Ti1–C3	2.460(13)	Ti3–Cl2	2.502(3)
Ti1–C4	2.503(12)	Ti3–Cl3	2.510(5)
Ti1–C5	2.493(12)	Ti3–Cl7	2.186(5)
Ti1–C6	2.502(12)	Ti3–Cl8	2.209(4)
Ti2–Cl1	2.454(4)	Ti3–Cl9	2.205(4)
Ti2–Cl2	2.472(5)	Ti–Cp1	2.058(12)
C5–Ti1–C6	34.0(4)	Cl12–Ti1–Cp1	115.8(4)
C4–Ti1–C5	32.1(4)	Cl11–Ti1–Cl12	102.6(2)
C3–Ti1–C4	34.1(4)	Cl10–Ti1–Cp1	115.0(4)
C2–Ti1–C3	32.4(4)	Cl10–Ti1–Cl12	102.2(2)
C1–Ti1–C6	32.4(4)	Cl10–Ti1–Cl11	103.5(2)
C1–Ti1–C2	32.4(4)		

[a] Cp indicates the centroid of the aromatic ring C1–C6.

(2) Å),[34] $[Ti(\eta^6\text{-}C_6Me_6)_2(\mu_2\text{-}AlCl_4)_2]$ (2.06 Å).[35] The associated $[Ti_2Cl_9]^-$ anion is a distorted bisoctahedron with the bridging chlorine longer [from 2.454(4) to 2.510(5) Å] than the terminal ones [from 2.186(5) to 2.220(5) Å], as described earlier.[36]

The high stability of **2** could explain the observed $TiCl_4$-assisted trimerization of but-2-yne. In addition, such a reaction may give

(33) Krasochka, O. N.; Shestakov, A. F.; Tairova, G. G.; Shvetsov, Y. A.; Kvashina, E. F.; Ponomarev, V. I.; Atovmyan, L. O.; Borod'ko, Y. G. *Khim. Fiz.* **1983**, *11*, 1459; *Chem. Abstr.* **1984**, *100*, 43387g.

(34) Blackburn, D. W.; Britton, D.; Ellis, J. E. *Angew. Chem., Int. Ed. Engl.* **1992**, *31*, 1495.

(35) Thewalt, U.; Österle, F. *J. Organomet. Chem.* **1979**, *172*, 317.

(36) Kistemacher, T. J.; Stucky, G. D. *Inorg. Chem.* **1971**, *10*, 122.

Table 4. Optimized Geometries at the SCF (MCPF) Level of TiF_3^+ and $TiCl_3^+$ with Bond Lengths in Å and Angles in deg

	basis set I	basis set II	basis set III	basis set IV
		TiF_3^+		
r(Ti–F)	1.712 (1.745)	1.712	1.696	1.677 (1.704)
∠(FTiF)	117.2 (113.3)	117.1	119.0	116.8 (113.8)
		$TiCl_3^+$		
r(Ti–Cl)	2.157(2.177)	2.154	2.122	2.107 (2.128)
∠(ClTiCl)	117.9 (112.0)	118.0	119.1	117.4 (112.9)

insight on the nature of the labile precursor **1**. The trimerization reaction was performed by adding an excess of $TiCl_4$ to a CH_2Cl_2 solution of but-2-yne. When the reaction was carried out in a NMR tube two singlets at 2.22 and 2.83 ppm were observed. We never saw the singlet at 2.75 ppm observed during the complexation of C_6Me_6 by $TiCl_4$. This might be because the pathways leading to **2** from C_6Me_6 and but-2-yne involve different intermediates.

$$3\text{Me-C}\equiv\text{C-Me} + 3\ TiCl_4 \rightarrow \underset{\mathbf{2}}{[(\eta^6\text{-}C_6Me_6)TiCl_3]^+}[Ti_2Cl_9]^- \quad (2)$$

Discussion

Though not one of our main objectives, the precursor of **2** was a point of interest. Kochi and co-workers[4] have proposed for **1** a structure which is closely related to the X_2–arene[37] and CX_4–arene[38] charge transfer complexes. With that hypothesis, the mechanism leading to **2** should be written as the following redox sequence:

$$TiCl_4 + C_6Me_6 \rightarrow \underset{\mathbf{1}}{[C_6Me_6\cdot TiCl_4]} \rightleftarrows C_6Me_6^{\bullet+} + Ti^{III}Cl_4^{\bullet-} \rightarrow [C_6Me_6^{\bullet+} + Ti^{III}Cl_3^{\bullet} + Cl^-] \rightarrow \underset{\mathbf{3}}{[(\eta^6\text{-}C_6Me_6)TiCl_3]^+}Cl^- \overset{TiCl_4}{\rightleftarrows} \underset{\mathbf{2}}{[(\eta^6\text{-}C_6Me_6)TiCl_3]^+}[Ti_2Cl_9]^- \quad (3)$$

Complex **1** may form by the direct binding of the arene to the metal or in an indirect way by recombination of the ions in **3**. Therefore the sequence leading to the formation of **2** can be simplified as reported in eq 4.

$$TiCl_4 + C_6Me_6 \rightleftarrows \underset{\mathbf{1}}{[C_6Me_6\cdot TiCl_4]} \rightleftarrows \underset{\mathbf{3}}{[(\eta^6\text{-}C_6Me_6)TiCl_3]^+}Cl^- \overset{TiCl_4}{\rightleftarrows} \underset{\mathbf{2}}{[(\eta^6\text{-}C_6Me_6)TiCl_3]^+}[Ti_2Cl_9]^- \quad (4)$$

The ^{1}H NMR spectrum of **2** dissolved in CD_2Cl_2 or the reaction of $TiCl_4$ with C_6Me_6 in CD_2Cl_2 (see Experimental Section and Results) showed essentially the same spectrum with the presence of three singlets. This seems to support well the multistade equilibrium reported in reaction 4. The singlet at 2.75 ppm can be tentatively assigned to **3**, containing C_6Me_6 bonded to the $[TiCl_3]^+$ cation, a chemical shift not so much different from that of **2** (2.83 ppm). An additional feature of the multistep equilibrium (4) is its dependence on the temperature, which is significantly shifted to the left with increasing temperatures. Increasing the temperature from 283 to 323 K, we observed the disappearance of the singlet at 2.75 and 2.83 ppm and a significant increase of the singlet at 2.22 ppm (free C_6Me_6). An interesting question arises on the nature of **1**.

The direct η^6-bonding of the arene to $TiCl_4$ have been simulated in a theoretical calculation and has been found to be energetically very unfavorable due to the high energy required to distort the tetrahedral geometry of $TiCl_4$ to a C_{4v} fragment (*vide infra*). Preserving the tetrahedral structure of $TiCl_4$ in presence of aromatic hydrocarbons favors a halogen-bonded *vs* metal-bonded charge transfer complex. The halogen-bonded complex is based on the structural model of CX_4–arene charge transfer complexes and not on metals having empty accessible d orbitals. We did not find any support for this model from a theoretical calculation (*vide infra*).

An energetically more favorable approach between $TiCl_4$ and an arene, supported by the calculations (*vide infra*), is a preliminary η^2 binding of the aromatic ring to the metal. This requires much less energy to distort the tetrahedral $TiCl_4$. An interaction between $TiCl_4$ and a single C–C multiple bond can be the first step in the $TiCl_4$-assisted stoichiometric trimerization of the but-2-yne, as reported in eq 5.

$$TiCl_4 + \text{Me-C}\equiv\text{C-Me} \longrightarrow \underset{\mathbf{A}}{\left[Cl_4Ti\left(\begin{matrix}Me\\ \|\\ Me\end{matrix}\right)\right]} \xrightarrow[TiCl_4\ (excess)]{\text{Me-C}\equiv\text{C-Me}} \underset{\mathbf{2}}{[(\eta^6\text{-}C_6Me_6)TiCl_3]^+}[Ti_2Cl_9]^- \quad (5)$$

We are not in the position, however, to detail the mechanism of reaction 5, except for the fact that such a mechanism should not require the intermediacy of **3** and **1**, which are the likely origin of the singlet in the ^{1}H NMR spectrum at 2.75 ppm.

Rare examples of metal halide promoted cyclooligomerization of internal acetylenes, i.e. but-2-yne, have been observed, making use of $AlCl_3$,[39] $NbCl_5$, and $TaCl_5$.[40] In spite of the impressive number of proposed mechanisms for acetylene cyclooligomerization, many of them are unappropriate in our case.[41] They involve the following: (i) changes in the oxidation state of the metal (oxidative addition, reductive elimination); (ii) preliminary insertion of the C–C triple bond into the Ti–Cl bond, a mechanism we ruled out in a detailed study of the reaction between $TiCl_4$ and isocyanides concerning the Passerini reaction;[42] (iii) the intermediate formation of a metalloalkylidene or -alkylidyne.

We undertook a theoretical study on the following model compounds:

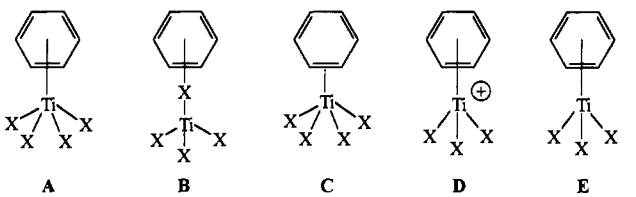

Compounds **A**, **B**, and **C** represent proposed precursors of the isolated **D** arene complex, while the as yet unknown titanium-

(37) Hassel, O.; Stromme, K. O. *Acta Chem. Scand.* (a) **1959**, *13*, 1781; (b) **1958**, *12*, 1146.
(38) Streiter, F. J.; Templeton, D. H. *J. Chem. Phys.* **1962**, *37*, 161.
(39) Schäfer, W. *Angew. Chem., Int. Ed. Engl.* **1966**, *5*, 669.
(40) (a) Dändliker, G. *Helv. Chim. Acta* **1969**, *52*, 1482. (b) Masuda, T.; Mouri, P.; Higashimura, T. *Bull. Chem. Soc. Jpn.* **1980**, *53*, 1152. *J. Chem. Soc., Chem. Commun.* **1982**, 1297.
(41) (a) Davidson, J. L. Reactions of Coordinated Acetylenes. In *Reactions of Coordinated Ligands*, Braterman, P. S., Ed.; Plenum: New York, 1986; Chapter 31, p 825. (b) Davies, S. G. *Organotransition Metal Chemistry: Applications to Organic Synthesis*; Pergamon: Oxford, U.K., 1982; pp 255–259. (c) Keim, W.; Behr, A.; Röper, M. In *Comprehensive Organometallic Chemistry*; Wilkinson, G., Stone, F. G. A., Abel, E. W., Eds.; Pergamon: Oxford, U.K., 1981; Vol. 8, Chapter 52. (d) Kochi, J. K. *Organometallic Mechanisms and Catalysis*, Academic: New York, 1978; p 428. (e) Shore, N. E. *Chem. Rev.* **1988**, *88*, 1081.
(42) Carofiglio, T.; Floriani, C.; Chiesi-Villa, A.; Rizzoli, C. *Organometallics* **1991**, *10*, 1659. Cozzi, P. G.; Carofiglio, T.; Floriani, C.; Chiesi-Villa, A.; Rizzoli, C. *Organometallics* **1993**, *12*, 2845.

Table 5. Minimum and Transition State of TiF_3^+ and $TiCl_3^+$, Evaluated Using BS4 with Bond Lengths in Å, Angles in deg, Absolute Energies in hartree, and Energy Differences in kcal mol^{-1}

	SCF			MCPF		
	minimum		transition state	minimum		transition state
			TiF_3^+			
r(Ti–F)	1.677		1.683	1.704		1.708
∠(FTiF)	116.8		120.0	113.8		120.0
energy	−1146.67582		−1146.67573	−1147.43476		−1147.43259
ΔE		0.1			1.4	
ΔE_{ZPEC}[a]		−0.1			1.2	
			$TiCl_3^+$			
r(Ti–Cl)	2.107		2.116	2.128		2.134
∠(ClTiCl)	117.4		120.0	112.9		120.0
energy	−2226.78562		−2226.78585	−2227.39314		−2227.39016
ΔE		−0.1			1.9	
ΔE_{ZPEC}[a]		−0.3			1.7	

[a] Zero point energy correction evaluated using the SCF vibrational frequencies of TiF_3^+.

Table 6. Optimized Geometries of the Investigated Systems with Bond Lengths in Å and Angles in deg[a]

	TiF_3^+	TiF_3	$TiCl_3^+$	$TiCl_3$
r(Ti–X)	1.712	1.816	2.157	2.275
∠(XTiX)	117.2	120.0	117.9	120.0
	$TiF_3C_6H_6^+$	$TiF_3C_6H_6$	$TiCl_3C_6H_6^+$	$TiCl_3C_6H_6$
r(Ti–C^n)[b]	2.269	2.887	2.275 (2.059)[c] 2.252[d]	2.767
		2.818[e]	2.249[e]	
r(Ti–X)	1.746	1.834	2.204 (2.179)[c]	2.310
∠(XTiX)	106.3	115.3	103.4 (102.7)[c]	111.9

[a] The optimized geometry of C_6H_6 is r(C–C) = 1.395 and r(C–H) = 1.072. [b] C^n refers to the centroid of C_6H_6. [c] Experimental geometry from ref 18. [d] Optimized value at CI level. [e] Optimized value at MCPF level.

Table 7. Binding Energies (Kcal mol^{-1}) of the $TiX_3C_6H_6^{0,+}$ Systems, Evaluated with Respect to $TiX_3^{0,+}$ and C_6H_6, in Their Ground State, Unless Otherwise Stated with Interaction Energies (kcal mol^{-1}) in Parentheses

	SCF	MCPF
$TiF_3C_6H_6^+$ ($^1A_1$)	66.0 (73.5)	66.3 (68.3)
$TiCl_3C_6H_6^+$ ($^1A_1$)	57.6 (66.2)	59.1 (61.6)
$TiF_3C_6H_6$ ($^2A_1$)	5.9 (11.8)	8.5 (13.2)
(^2E)[a]	8.6 (15.4)	
$TiCl_3C_6H_6$ ($^2A_1$)	4.9 (15.1)	8.9 (17.8)
(^2E)[a]	8.2 (18.3)	

[a] Binding energy evaluated with respect to the TiX_3 $^2E''$ correlating asymptotic state.

(III) arene complex **E** may be a player in some of the $TiCl_4$–arene redox processes.

Theoretical Calculations

Table 4 shows the optimized geometries of TiF_3^+ and $TiCl_3^+$, while Table 5 shows both the minima and the saddle points of these species. Table 6 shows the optimized geometries of the investigated complexes, Table 7 the binding energies evaluated as energy differences between the energy of the $TiX_3C_6H_6^{0,+}$ complex and those of the separated $TiX_3^{0,+}$ and C_6H_6 fragments, all of them in their optimized geometry. Table 7 reports also the interaction energies evaluated considering the complex in its optimized geometry and the fragments in the same geometry they show in the complex.

Let us start our analysis with the description of the structures of TiF_3^+ and $TiCl_3^+$. This point will be helpful in the following description of the bonding in the investigated complexes.

Ground-State Geometries and Inversion Barriers for TiF_3^+ and $TiCl_3^+$. Table 4 shows the optimized geometries of TiF_3^+ and $TiCl_3^+$ evaluated at SCF level by means of gradient techniques, using several basis sets.

Both TiF_3^+ and $TiCl_3^+$ show a pyramidal structure with a small deviation from planarity (basis **I**). The addition of diffuse functions to improve the description of the fluorine and chlorine atoms, which carry a consistent negative charge as suggested by the Mulliken analysis, has a negligible effect on the geometry (basis **II**). More pronounced, as expected, are the differences in the geometries evalulated using basis **III**, *i.e.* a basis set of triple-ζ valence plus polarization quality. We have a decrease in the r(Ti–X) bond length and a slight increase in the ∠(XTiX) angle. The improved description of the titanium atom (basis **IV**) has mainly the effect of a decrease in ∠(XTiX). Force constants calculations, performed using both basis **I** and **III**, confirmed that the stationary points localized on the potential energy surface are true minima.

The inclusion of correlation effects (basis **I** and **IV**) implies a lengthening of r(Ti–X) and a more consistent decrease in ∠(XTiX). Our calculations suggest that both TiF_3^+ and $TiCl_3^+$ are nonplanar, although the deviation from planarity is not very pronounced. This geometry is the result of a compromise between ligand–ligand repulsion, which would lead to a planar structure, and the overlap between ligand and metal orbitals, which is larger for a nonplanar structure due to symmetry reasons (in C_{3v} all the Ti d orbitals may overlap with ligand orbitals, while in D_{3h} only three Ti d orbitals may overlap). Ligand to metal π-bonding does not seem to be so relevant. Ligand–ligand repulsion is well described also at the SCF level, while metal–ligand bonding needs the inclusion of correlation to be properly described. For this reason the SCF has a bias toward an almost planar structure.

For comparison purposes comparable calculations have been performed on TiH_3^+, using basis **I**. The optimized geometry at SCF level is r(Ti–H) = 1.624 Å and ∠(HTiH) = 94.6°. The bonding in this molecule is completely comparable to that found in TiF_3^+ and $TiCl_3^+$: the angle ∠(HTiH) is much smaller than ∠(FTiF) and ∠(ClTiCl) only because of the less pronounced ligand–ligand repulsion.

Table 5 shows the minimum and transition state geometries and energies of TiF_3^+ and $TiCl_3^+$, evaluated using basis **IV**, both at the SCF and MCPF level of theory. An estimate of the zero-point energy has been performed using the vibrational frequencies of TiF_3^+, calculated at the SCF level with basis **III**.

At the SCF level the difference between planar and nonplanar structures is negligible due to the overestimation of ligand–ligand repulsion with respect to metal–ligand bonding. Conversely, the inclusion of correlation effects improving the description of metal–ligand bonding clearly shows that the structures of TiF_3^+ and $TiCl_3^+$ are nonplanar, the inversion barrier being, however, only 1.2 and 1.7 kcal mol^{-1}, respectively.

Interaction between TiX_3^+ and C_6H_6. The interaction of TiX_3^+ with benzene implies a lengthening of r(Ti–X) of 0.03–0.05 Å and a decrease in ∠(XTiX), *i.e.* an increase in the deviation from

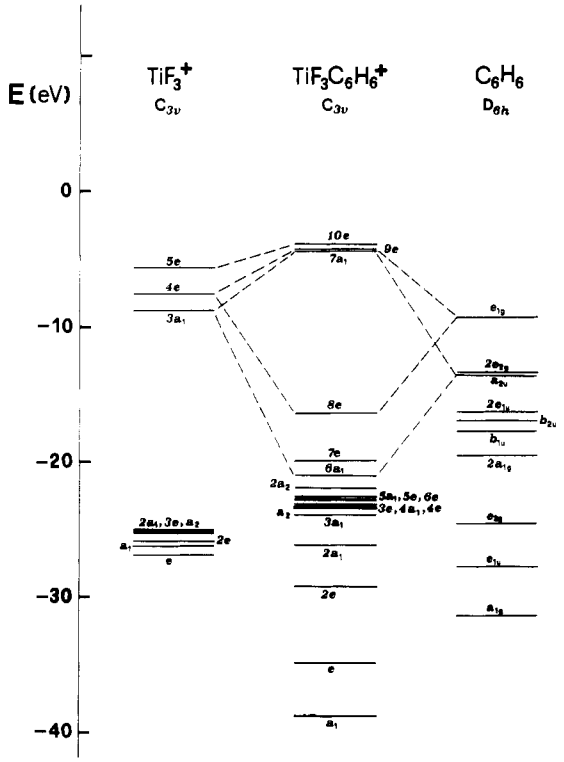

Figure 3. Molecular-orbital correlation diagram of $[TiF_3C_6H_6]^+$.

planarity, more pronounced for $TiCl_3^+$. A comparison with experimental data is possible between the optimized structure of $TiCl_3C_6H_6^+$ and the X-ray structure of $[(\eta^6\text{-}C_6Me_6)TiCl_3]^+[Ti_2Cl_9)]^-$.[8] The r(Ti–Cl) and ∠(ClTiCl) parameters are in very good agreement (see Table 6), while r(Ti–C^n), *i.e.* the distance between the titanium atom and the centroid of the arene molecule, differs by as much as 0.216 Å. In order to check if this difference could be due to limits in our treatment, we reoptimized this parameter at both Cl and MCPF levels of theory, keeping the other geometrical parameters fixed at their optimized SCF values. The inclusion of correlation effects implies a very small shortening (less than 0.03 Å) of the r(Ti–C^n) distance. The difference between the theoretical and experimental values, therefore, should be ascribed mainly to the different chemical behavior of C_6H_6 and C_6Me_6, although some difference could be due also to solid-state forces.

In preliminary calibration calculations, we have performed a full geometry optimization of $TiCl_3C_6H_6^+$. The optimization of the C_6H_6 geometry coupled to the variation of the other geometrical parameters implied a lowering in the energy of only 0.9 kcal mol^{-1}. For this reason we kept frozen the C_6H_6 geometrical parameters in all the subsequent calculations.

The bonding between TiX_3^+ and C_6H_6 is primarily due to charge-induced dipole interactions and this is confirmed by the very small geometry variation of the benzene molecule upon bond formation: in $TiCl_3C_6H_6^+$ the r(C–C) bond distance is increased by only 0.011 Å, while r(C–H) is shortened by 0.003 Å. Together with the electrostatic contribution, however, there is also benzene π to metal d donation and metal d to benzene π^* back-donation, which are possible mechanisms to increase the strength of the bonding when transition metals are involved.

A useful, although qualitative, way of interpreting the nature and origin of the bonding is provided by the analysis and correlation of the molecular orbitals (MOs) of the fragments and the complex. The analysis of the molecular orbitals of $TiF_3C_6H_6^+$ shows that the main bonding orbitals between TiF_3^+ and C_6H_6 are the $6a_1$ and 8e, as we can see from Figure 3, where we have reported a molecular-orbital correlation diagram, where only the main correlations are shown. These orbitals derive from the interaction between the π orbitals of C_6H_6 (a_{2u} and e_{1g}) and virtual orbitals of TiF_3^+ of mainly Ti character. In particular, the $6a_1$ MO originates from the interaction between C_6H_6 a_{2u} and TiF_3^+ $3a_1$, which is mainly Ti s, p_z, and d_{z^2}. The 8e MO may be viewed as the interaction between C_6H_6 e_{1g} and TiF_3^+ 4e, which is essentially Ti d_{xz} and d_{yz}. Both these interactions imply a donation of electron density from benzene to TiF_3^+. The metal d to benzene π^* back-donation is almost absent since the Ti d_{xy} and $d_{x^2-y^2}$ orbitals, which could donate to the benzene e_{2u} orbitals are involved in the bonding with the fluorine atoms and strongly polarized towards them.

This picture of the bonding is confirmed by the results of the Mulliken population analysis which shows that the population of C does not change appreciably upon bond formation, since the decrease in C π electron density is compensated for by a decrease in the population of the hydrogen atoms, which become the electrophilic centers in the aromatic ring.

A comparable picture holds for the bonding in $TiCl_3C_6H_6^+$. The main bonding orbitals originate from the interaction of C_6H_6 π MOs and $TiCl_3^+$ virtual MOs of mainly Ti character, with only a small contribution of chlorine. In agreement with the bonding picture the Mulliken population analysis shows a charge transfer from C_6H_6 to $TiCl_3^+$, which is slightly larger than that observed in the corresponding fluorine complex, although also metal d to benzene π^* back-donation is larger, the decrease in the Ti d_{xy} and $d_{x^2-y^2}$ populations being 0.22 e. By contrast, the net positive charge on Ti is much lower in $TiCl_3C_6H_6^+$ than in $TiF_3C_6H_6^+$, suggesting that the electrostatic contribution to the bonding is weaker in the chlorine complex than in the fluorine one. It is worthwhile to note that also in $TiCl_3C_6H_6^+$ the decrease in the C π electron densities is compensated for by a decrease in the H populations, with the result that we do not have variation in the global C population upon bond formation. The hydrogen atoms are the electrophylic centers also in this compound.

The binding energy between TiX_3^+ and C_6H_6 is computed to be 66.0 and 57.6 kcal mol^{-1} (see Table 7) for the fluorine and chlorine systems, respectively, at the SCF level of theory. The strength of the bonding, however, is better described by the interaction energy, evaluated as the energy difference between the complex in its optimized geometry and the fragments in the same geometry they present in the complex. The interaction energies are computed to be 73.5 and 66.2 kcal mol^{-1} for the fluorine and chlorine compound, respectively. The bonding with benzene is stronger for TiF_3^+ than for $TiCl_3^+$.

Since the difference in the binding energies is small, correlation effects may play a fundamental role and even reverse the relative stabilities of the analysed systems. For this reason calculations with inclusion of correlation have been performed on the investigated systems. Since the SCF occupation is a good zeroth-order representation of the analyzed systems, SCF-based MCPF calculations have been performed on the complexes and the separated fragments, using the SCF optimized geometries.

The description of the bonding between TiX_3^+ and C_6H_6 at the MCPF level of theory is entirely comparable to that obtained at the SCF level.

The binding (interaction) energies at the MCPF level are computed to be 66.3 (68.3) and 59.1 (61.6) kcal mol^{-1} for $TiF_3C_6H_6^+$ and $TiCl_3C_6H_6^+$, respectively. These values are very close to those obtained at the SCF level confirming that the SCF wave function is a good representation of these systems. The binding energies evaluated at the MCPF level, however, are underestimates of the "true" binding energy, since they are evalulated considering the SCF-optimized geometry for the complex and the MCPF optimized geometry for the fragments. This underestimation, however, should be partly cancelled by the basis set superposition error.

At this point we can summarize our results: TiF_3^+ gives rise to a stronger bond with C_6H_6 than $TiCl_3^+$ mainly because of the stronger electrostatic interaction. The ligand to metal donation strengthens the bonding while the metal to ligand back-donation is almost absent. This is different than in $TiC_6H_6^+$, where very accurate calculations[43] have recently shown that metal to ligand π^* donation is an important contribution to the bonding. This difference can be easily understood if we consider the ionization potentials (IPs) of the species involved in the bonding. The IPs of Ti, $TiCl_3$, and TiF_3 are computed to be 5.96, 9.17, and 9.81 eV, at the MCPF level. The vertical IP of C_6H_6 is computed to be 8.95 eV (the adiabatic IP is of course smaller than this value). In a charge exchange reaction ($M^+ + L \rightarrow M + L^+$), it is assumed that transfer occurs if the IP of the ligand is smaller than that of the metal. This is the case for $TiCl_3^+$ and TiF_3^+ but not for Ti^+. The IPs show also that $TiCl_3$ and TiF_3 can be classified as Lewis acids with respect to C_6H_6, while Ti(0) is a Lewis base.

Interaction between TiX_3 and C_6H_6. TiF_3 and $TiCl_3$ show a planar structure, as can be seen from Table 6. The ground state of both molecules is computed to be $^2A'_1$, with the unpaired electron in a a'_1 MO of mainly Ti d_{z^2} character. This orbital is perpendicular to the plane of the TiX_3 molecule: TiF_3 and $TiCl_3$ are planar in order to minimize the repulsion between the negatively charged X ligands and the electron density localized in the Ti d_{z^2} orbital. The r(Ti–F) bond length is in excellent agreement with that computed in the near-Hartree–Fock calculations of Yates and Pitzer.[44]

The interaction of TiX_3 with benzene implies a lengthening of r(Ti–X) of 0.02–0.04 Å and a decrease in $\angle$(XTiX), more pronounced for $TiCl_3$. The r(Ti–C^n) bond length, *i.e.* the distance between the titanium atom and the centroid of C_6H_6, is computed to be 2.887 and 2.767 Å for fluorine and chlorine compounds, respectively. These values are much longer than the corresponding ones of the cationic species and suggest the presence of a much weaker bond in the neutral systems. The r(Ti–C^n) distance in $TiCl_3C_6H_6$ is shorter than that in $TiF_3C_6H_6$ by 0.12 Å. This suggests the presence of a stronger bond in the chlorine compound, *i.e.* a reversed situation with respect to the cationic species. The r(Ti–C^n) bond length in $TiF_3C_6H_6$ has been optimized also at the MCPF level of theory, keeping the other geometrical parameters fixed at their optimized SCF values. The inclusion of correlation effects implies a small shortening of r(Ti–C^n) by only 0.07 Å, suggesting that the SCF-optimized geometries are reliable.

The analysis of the molecular orbitals of $TiF_3C_6H_6$ shows that the bonding between TiF_3 and C_6H_6 is described mainly by the $6a_1$ and 8e MOs, as can be seen from Figure 4, where we have reported a molecular orbital correlation diagram. In order to simplify the correlation, the molecular orbital energy levels of TiF_3 in a C_{3v} geometry (*i.e.* in the same geometry as in the complex) have been reported. The $6a_1$ and 8e MOs derive from the interaction of C_6H_6 π orbitals with virtual orbitals of TiF_3 with mainly Ti character. These orbitals, however, are mainly localized on benzene, with only a small contribution from titanium and this suggests the presence of a weak interaction between the metal fragment and the aromatic ring. The $6a_1$ MO derives from the interaction between C_6H_6 a_{2u} and a virtual orbital of TiF_3^+ with mainly Ti p_z, and d_{z^2} character, while the 8e MO originates from the interaction between C_6H_6 e_{1g} and a virtual orbital of TiF_3 of mainly Ti d_{xz} and d_{yz} character. Both these orbitals imply a donation of electron density from the benzene molecule to the metal fragment. This picture of the bonding is confirmed by the results of the Mulliken population analysis, which shows an increase in the electron density of TiF_3 (of 0.11 e) and a decrease in the electron density of C_6H_6, upon bond formation. The net charge transfer from C_6H_6 to TiF_3, however, is much smaller in

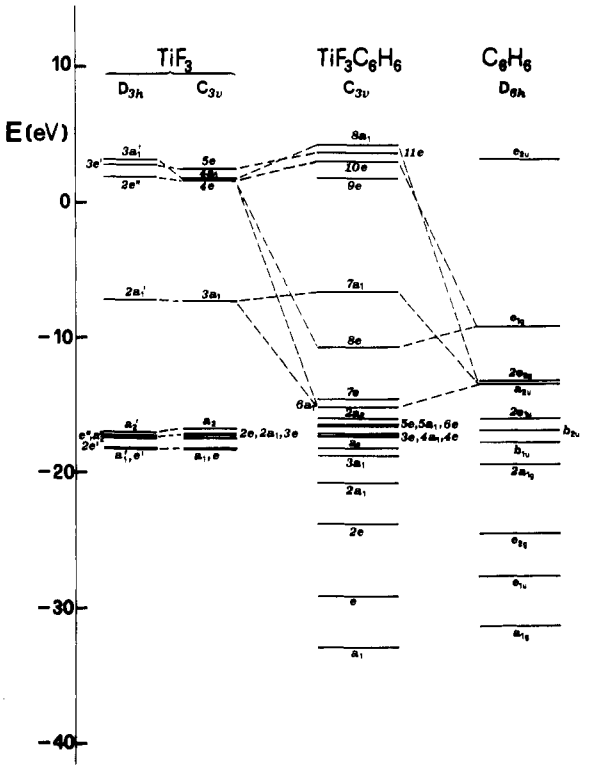

Figure 4. Molecular-orbital correlation diagram of $[TiF_3C_6H_6]$.

$TiF_3C_6H_6$ than in $TiF_3C_6H_6^+$ suggesting, once again, the presence of a weaker interaction in the neutral system. The Mulliken analysis shows the presence of a positive charge on the titanium atom (+1.72 at the SCF level; +1.21 at the MCPF level), although the TiF_3 fragment in the complex is negatively charged. This point indicates the presence of an electrostatic contribution to the bonding, through a dipole-induced dipole interaction.

A comparable picture holds for the description of the bonding in $TiCl_3C_6H_6$. From the Mulliken population analysis for $TiCl_3C_6H_6$ we can see, however, a large charge transfer from C_6H_6 to $TiCl_3$, with respect to the fluorine compound (0.21 and 0.11 e, respectively). $TiCl_3$ is, therefore, a stronger Lewis acid than TiF_3: this trend in the relative acid strength is analogous to that experimentally observed for BF_3 and BCl_3,[45] in contrast to the classically expected order based on electronegativity.

The binding energy between TiX_3 and C_6H_6 is computed to be 5.9 and 4.9 kcal mol^{-1} for the fluorine and chlorine compound, respectively, at the SCF level of theory (Table 7). The binding energy is the sum of the interaction energy and the deformation energy of the ligands, *i.e.* the energy required by the ligands to reach the "optimum" geometry for their interaction. The deformation energy is computed to be 5.9 and 10.2 kcal mol^{-1} for $TiF_3C_6H_6$ and $TiCl_3C_6H_6$, respectively. As a result, the interaction energy is 11.8 and 15.1 kcal mol^{-1} for the fluorine and chlorine compound, respectively. $TiCl_3$ shows a stronger interaction with C_6H_6 than TiF_3, due to its higher Lewis acidity. It is interesting to notice that the binding energy computed in the first excited state (^2E), evaluated with respect to the TiX_3 $^2E''$ correlating asymptotic state, is larger than that relative to the ground state ($^2A_1$) for both the fluorine and chlorine systems. In the ^2E state the unpaired electron is in an orbital which is essentially Ti d_{xz} and d_{yz} in character, while in the $^2A_1$ state the unpaired electron is in the Ti d_{z^2} orbital. The occupation of this orbital implies a strong repulsion with the C_6H_6 π electron density. This explains the weakness of the bonding in $TiF_3C_6H_6$ and $TiCl_3C_6H_6$ and the

(43) Bauschlicher Jr., C. W.; Partridge, H.; Langhoff, S. R. *J. Phys. Chem.* **1992**, *96*, 3273.
(44) Yates, J. H.; Pitzer, R. M. *J. Chem. Phys.* **1979**, *70*, 4049.
(45) Brown, H. C.; Holmes, R. H. *J. Am. Chem. Soc.* **1956**, *78*, 2173. Bax, C. M.; Katritzky, A. R.; Sutton, L. E. *J. Chem. Soc.* **1958**, 1258. Lappert, M. F. *J. Chem. Soc.* **1962**, 542.

Table 8. C_6H_6 π and $TiX_3^{0,+}$ LUMO Orbital Energies (eV) and Energy Gaps (eV) between the Interacting Orbitals

	a_{2u}		e_{1g}	
C_6H_6	−13.74		−9.25	
	d_σ	$\Delta(a_{2u}-d_\sigma)$	d_π	$\Delta(e_{1g}-d_\pi)$
TiF_3^+	−8.68	5.06	−7.60	1.65
$TiCl_3^+$	−7.63	6.11	−7.09	2.16
TiH_3^+	−5.25	8.49	−5.11	4.14
$TiCl_3$	2.75	16.49	0.62	9.87
TiF_3	3.18	16.92	1.91	11.16

long bond length between Ti and benzene in these compounds. The promotion of the unpaired electron to an orbital not directly pointing toward the aromatic ring reduces this repulsion and gives rise to a larger interaction energy. This problem has been clearly explained by Bauschlicher and co-workers.[46] The gain in the interaction energy, however, is not enough to compensate the promotion energy required by the TiX_3 fragment to go from the $2A'$ ground state to the $2E''$ first excited state, leaving the 2E state of the complex above the $2A_1$ one.

The influence of the electron repulsion on the strength of the interaction between Ti and benzene has been investigated also by performing calculations on $TiCl_4C_6H_6$. Two geometries of $TiCl_4C_6H_6$ have been analyzed: a trigonal bipyramid and a square base pyramid with the benzene at the apex site. For the first geometry no minima have been localized in the potential energy surface, while for the second one a minimum with the following geometrical parameters have been found: r(Ti–Cl) = 2.313 Å, r(Ti–cp) = 2.642 Å, $\angle$(ClTi(cp)) = 104.1°. The interaction energy between $TiCl_4$ and C_6H_6 at the SCF level is 21.5 kcal mol^{-1}: $TiCl_4$ gives rise to a stronger interaction with C_6H_6 than $TiCl_3$ due to the reduced electron repulsion. Indeed, $TiCl_4$ has all the metal valence electrons involved in the bonding with the chlorine atoms, while $TiCl_3$ has a nonbonding valence electron which interacts strongly with C_6H_6. The energy required by $TiCl_4$ to reach the bonding geometry, however, is very high, the deformation energy being 62.6 kcal mol^{-1}. This energy is not compensated for by the interaction energy and, as a result, $TiCl_4$ and C_6H_6 are unbound at least as far as Cl_4Ti–(η^6-C_6H_6) coordination is considered.

The interaction between C_6H_6 and $TiCl_4$ with a chlorine atom pointing toward the center of the arene ring has been as well investigated. This interaction, however, is repulsive at any bonding distance.

A completely different picture holds if we consider the benzene ring approaching $TiCl_4$ in a η^2-fashion and leading formally to [(η^2-C_6H_6)$TiCl_4$].

We optimized the distance between the titanium atom and the midpoint of a C=C bond (X), keeping the geometries of $TiCl_4$ and C_6H_6 fixed at their equilibrium values. We found the presence of a stable adduct at a distance Ti–X of 4.450 Å, the stabilization energy being 2.0 kcal mol^{-1}. This adduct can be a plausible precursor of the really isolated $[(\eta^6\text{-}C_6Me_6)TiCl_3]^+[Ti_2Cl_9]^-$ complex,[8] which could be formed by the action of $TiCl_4$ on this initially formed [$TiCl_4(\eta^2$-$C_6H_6)$] adduct.

The inclusion of correlation effects through MCPF calculations increases slightly both the binding and the interaction energies (8.5 and 13.2 kcal mol^{-1} for $TiF_3C_6H_6$; 8.9 and 17.8 kcal mol^{-1} for $TiCl_3C_6H_6$). These values, moreover, are underestimates of the "true" binding energy, since they are evaluated considering the SCF-optimized geometry for the complex and the MCPF optimized geometry for the separated fragments. The correlation effects, however, do not change appreciably the description of the bonding in the investigated systems and confirm that $TiCl_3$ is a stronger Lewis acid than TiF_3.

(46) Bauschlicher Jr, C. W.; Langhoff, S. R. *Int. Rev. Phys. Chem.* **1990**, *9*, 149.

Table 9. Optimized Geometries and Relative Energies[a] for the Trimerization of Acetylene with Bond Lengths in Å, Angles in deg, and Energies in kcal mol^{-1}

	acetylene	transition state	benzene
r(C=C)	1.202	1.232	1.395
r(C···C)	∞	2.219	1.395
r(C—H)	1.054	1.055	1.072
$\angle$(CCH)	180.0	151.9	120.0
energy	0	59.9	−129.9

[a] Relative to three times the total energy of acetylene.

Acid Strength of $TiX_3^{0,+}$. The energies for the interaction of $TiX_3^{0,+}$ with C_6H_6 suggest the following trend in the acid strength of $TiX_3^{0,+}$:

$$TiF_3^+ > TiCl_3^+ \gg TiCl_3 > TiF_3$$

This trend should be related both to the net charge transfer (Q_{CT}) from the donor to the acceptor ligand and to the geometry deformation of the ligands. Q_{CT}, as derived from the Mulliken population analysis, is computed to be 0.68 e for TiF_3^+, 0.71 e for $TiCl_3^+$, 0.11 e for TiF_3, and 0.23 e for $TiCl_3$. The difference in Q_{CT} between TiF_3^+ and $TiCl_3^+$ is only 0.03 e. Owing to the uncertainty of the Mulliken population analysis method, we cannot make any considerations on the relative acid strength of TiF_3^+ and $TiCl_3^+$ based only on Q_{CT}.

The charge transfer is related to the structural changes that occur in the acceptor upon complex formation. From the values reported in Table 6, we can compute the change in $\angle$(XTiX) [Δ(XTiX)] upon bond formation. Δ(XTiX) is 10.9° for TiF_3^+, 14.5° for $TiCl_3^+$, 4.7° for TiF_3, and 8.1° for $TiCl_3$, in agreement with the Q_{CT} trend. Both Q_{CT} and Δ(XTiX) therefore suggest the following trend in the acid strength of the investigated species:

$$TiCl_3^+ > TiF_3^+ \gg TiCl_3 > TiF_3$$

with an inversion with respect to the interaction energies between TiF_3^+ and $TiCl_3^+$. A recent MO study[47] on the relative Lewis acidity of BF_3 and BCl_3 suggests that the concept of charge transfer should be considered together with the concept of charge capacity,[48] i.e. the ability to accept the charge by the Lewis acid, in order to explain the observed trends in Lewis acidity. The electron affinities of TiF_3^+ and $TiCl_3^+$ are estimated to be 9.81 and 9.17 eV, at the MCPF level of theory: these values show a better ability to accept the charge by TiF_3^+ and $TiCl_3^+$ in perfect agreement with their relative Lewis acidity.

The bonding between $TiX_3^{0,+}$ and C_6H_6 can be described, besides the electrostatic contribution, as the interaction of C_6H_6 π orbitals and virtual orbitals of $TiX_3^{0,+}$ of mainly character Ti d_{z^2}, d_{xz}, d_{yz}. A good criterion for an estimate of the strength of this interaction and the acid strength of the acceptor ligand is given, therefore, by the energy gap between these overlapping orbitals. Table 8 shows the orbital energies of C_6H_6 MOs (a_{2u} and e_{1g}) and $TiX_3^{0,+}$ virtual orbitals of mainly character Ti d_{z^2} (d_σ) and Ti d_{xz}, d_{yz} (d_π), together with the energy gaps between them (Δ). Both $\Delta(a_{2u}-d_\sigma)$ and $\Delta(e_{1g}-d_\pi)$ show the increasing order

$$TiF_3^+ < TiCl_3^+ \ll TiCl_3 < TiF_3$$

in perfect agreement with the interaction energies.

In order to complete our analysis, we have performed SCF calculations also for the interaction between TiH_3^+ and C_6H_6. As

(47) Brinck, T.; Murray, J. S.; Politzer, P. *Inorg. Chem.* **1993**, *32*, 2622.
(48) Huheey, J. E. *J. Phys. Chem.* **1965**, *69*, 3284. Huheey, J. E.; Watts, J. C. *Inorg. Chem.* **1973**, *10*, 1553. Politzer, P. *J. Chem. Phys.* **1987**, *86*, 1072. Politzer, P.; Huheey, J. E.; Murray, J. S.; Grodzicki, M. *J. Mol. Struct. THEOCHEM* **1992**, *97*, 259.

Table 10. Optimized Geometries and Relative Energies[a] for the Trimerization of Acetylene, Promoted by $TiCl_3^+$ with Bond Lengths in Å, Angles in deg, Energies in kcal mol^{-1}

	$TiCl_3^+ + C_2H_2$	$TiCl_3C_2H_2^+$	$TiCl_3(C_2H_2)_2^+$	transition state	$TiCl_3C_6H_6^+$
r(C═C)	1.202	1.212	1.207	1.234	1.406
r(C···C)	∞	∞	3.414	2.248	1.406
r(C—H)	1.054	1.064	1.060	1.059	1.069
∠(CCH)	180.0	173.0	173.5	151.3	120.0
$\angle\beta$[b]		90.0	38.5	5.4	0.0
r(Ti—C)	∞	2.536	2.844	2.786	2.676
r(Ti—Cl)	2.157	2.171	2.185	2.208	2.204
∠(ClTiCl)	117.9	113.0	103.5	99.1	103.4
energy	0[c]	−39.3[d]	−43.6[e]	−6.6	−195.9

[a] Relative to the total energy of $TiCl_3^+$ plus three times the total energy of acetylene. [b] Angle between the C_2H_2 plane and the plane perpendicular to the C_3 axis of $TiCl_3^+$. The hydrogen atoms are pointing away from $TiCl_3^+$. [c] Energy of $TiCl_3^+ + 3C_2H_2$. [d] Energy of $TiCl_3C_2H_2^+ + 2C_2H_2$. [e] Energy of $TiCl_3(C_2H_2)_2^+ + C_2H_2$.

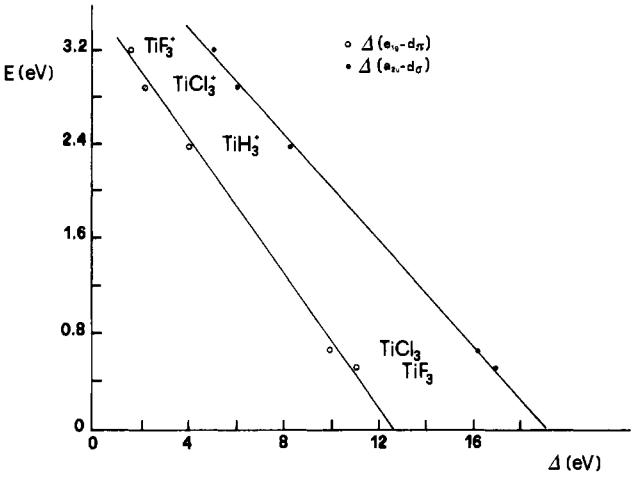

Figure 5. Interaction energy as a function of the overlapping orbital energy gaps for the analyzed systems.

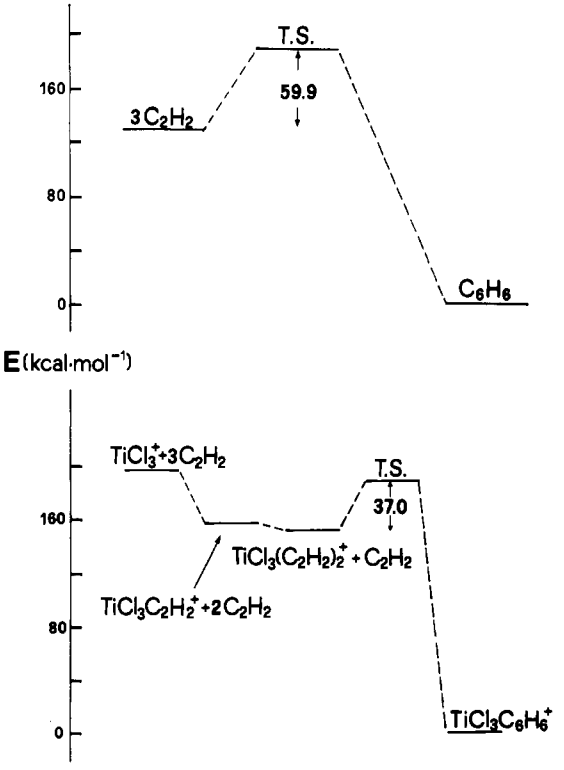

Figure 6. Surfaces for acetylene trimerization.

already observed for the fluorine and chlorine compounds, also for $TiH_3C_6H_6^+$ we have a lengthening of r(Ti–H) upon bond formation (by 0.032 Å). The r(Ti–C^n) bond distance is computed to be 2.298 Å and is longer than that computed for TiF_3^+ and $TiCl_3^+$, but much shorter than that evaluated for TiF_3 and $TiCl_3$. In agreement with this point, the binding (interaction) energy [53.6 (54.6) kcal mol^{-1}] is smaller than that computed for the cationic fluorine and chlorine compounds and suggests that TiH_3^+ is a weaker Lewis acid than TiF_3^+ and $TiCl_3^+$. The charge transfer Q_{CT} deduced from the Mulliken analysis, which is 0.60 e, and the Δ orbital energy gaps, shown in Table 8, are in agreement with this trend in the Lewis acid strength.

Figure 5 reports the interaction energy of $TiX_3^{0,+}$ with C_6H_6 as a function of the Δ values shown in Table 8. For both $\Delta(e_{1g} - d_\pi)$ and $\Delta(a_{2u} - d_\sigma)$ we have a linear correlation which makes evident this order in the strength of the interaction with benzene:

$$TiF_3^+ > TiCl_3^+ > TiH_3^+ \gg TiCl_3 > TiF_3$$

Moreover, we can have an estimate of the interaction energy in the complex once we have known the orbital energies of the fragments, at least as far as the bonding mechanism is the same.

Trimerization of Acetylene Promoted by Lewis Acids. The trimerization of acetylene to form benzene, although quite exothermic ($\Delta H° = -143$ kcal mol^{-1}), has a prohibitive activation energy.[49]

In order to understand the difference between the metal-promoted and the nonassisted reaction, we have investigated the reaction of trimerization of acetylene in the presence and in the absence of a promoter like $TiCl_3^+$. We observed that $TiCl_4$ promotes the trimerization of but-2-yne *via* the intermediacy of **2**.

Table 9 shows the optimized geometries and relative energies for this reaction without a promoter. At the transition state, the C≡C triple bond is only slightly elongated, while the C···C emerging bond is still very long. More consistent is the variation of the ∠(CCH) angle. However, we can classify this transition state as an early transition state. The exohergicity of the reaction is 129.9 kcal mol^{-1}, while the barrier height is 59.9 kcal mol^{-1}. The presence of this barrier has been attributed previously[49,50] both to geometry deformation and closed-shell repulsion between filled π-orbitals. Our calculations confirm this interpretation. Our calculated barrier height (59.9 kcal mol^{-1}), which is in very good agreement with the best estimate of Bach *et al.*[50] (61.6 kcal mol^{-1}), confirms however that the trimerization reaction cannot take place easily.

Let us investigate the reaction in the presence of $TiCl_3^+$. Table 10 shows the optimized geometries and relative energies for the trimerization of acetylene promoted by $TiCl_3^+$. The interaction of C_2H_2 with $TiCl_3^+$ gives rise to the stable species $TiCl_3C_2H_2^+$. The bonding between $TiCl_3^+$ and C_2H_2 is essentially electrostatic in origin, being due to charge-induced dipole interactions. This is clearly shown by the very little change in the acetylene geometry

(49) Houk, K. N.; Gandour, R. W.; Strozier, R. W.; Rondan, N. G.; Paquette, L. A. *J. Am. Chem. Soc.* **1979**, *101*, 6797 and references therein.
(50) Bach, R. D.; Wolber, G. J.; Schlegel, H. B. *J. Am. Chem. Soc.* **1985**, *107*, 2837.

upon bond formation.[51] The binding energy is computed to be 39.3 kcal mol^{-1}.

The approach of a second molecule of C_2H_2 gives rise to $TiCl_3(C_2H_2)_2^+$. The second molecule of acetylene is bound by only 4.3 kcal mol^{-1}, due to ligand–ligand repulsion. The approach of a third molecule of acetylene does not give rise to a stable structure since ligand–ligand repulsion overcompensates the gain in energy due to the electrostatic bondings. We have instead the transition state which leads to the benzene compound. The transition state shows a geometry very close to that evaluated for the transition state of the uncatalyzed reaction. The energy required for the geometry deformation and the electron repulsion is comparable in both reactions, but in the presence of $TiCl_3^+$ this energy is provided by the electrostatic interactions with $TiCl_3^+$. In this latter case the transition state is 6.6 kcal mol^{-1} under the reagents. In the presence of $TiCl_3^+$, therefore, there is no barrier for the reaction

$$TiCl_3^+ + 3\ C_2H_2 \rightarrow TiCl_3C_6H_6^+$$

Figure 6 summarizes our results. The trimerization of acetylene to benzene, although well exothermic does not happen easily due to a barrier as high as 59.9 kcal mol^{-1}. The same reaction promoted by $TiCl_3^+$ proceeds easily to the formation of the product directly or through acetylene complexes of $TiCl_3^+$.

(51) Sodupe, M.; Bauschlicher Jr, C. W. *J. Phys. Chem.* **1991**, *95*, 8640.

Conclusions

The reaction of $TiCl_4$ with C_6Me_6 under appropriate conditions led to the isolation of a d^0 metal–arene complexes. These results are relevant for the following reasons:

(i) We can promote the electrophilic activation of arenes using $TiCl_4$. The methyl protons are significantly shifted upfield from 2.22 to 2.80 ppm in complexes **2**, **5**, and **6**; the theoretical calculations showed a significant positive charge density on the protons of $[(\eta^6\text{-}C_6H_6)TiX_3]^+$ (X = F, Cl). (ii) The strong acid $[TiCl_3]^+$, which is much more acidic than $TiCl_4$, is available in the form of $[(\eta^6\text{-}C_6Me_6)TiCl_3]^+$, since the arene ligand is supposed to be easily displaced in complexes **2**, **5**, and **6**. (iii) $TiCl_4$ can be used as a promoter for the cyclotrimerization of electron-rich internal acetylenes.

Acknowledgment. We thank the Fonds National Suisse de la Recherche Scientifique (Grant No. 20-33420-92) and COST (European Cooperation Program) for financial support. The present work has been carried out within the "Progetto Finalizzato CNR *Materiali Speciali per Tecnologie Avanzate*". The authors would like to thank the CINECA for providing a computer grant.

Supplementary Material Available: Details of the CI and MCPF calculations (Table S1), experimental data for X-ray diffraction study, fractional atomic coordinates for hydrogen atoms, anisotropic thermal parameters, and bond distances, and angles for complex **2** (Tables S2–S5), and details of the theoretical calculations (Tables S8–S12) (14 pages). Ordering information is given on any current masthead page.